HAL
open science

Mode of action of the natural herbicide radulanin A as an inhibitor of photosystem II

Simon Thuillier, Stefania Viola, Bruce Lockett-Walters, Bastien Nay, Benjamin Bailleul, Emmanuel Baudouin

▶ To cite this version:

HAL Id: hal-04124088
https://hal.sorbonne-universite.fr/hal-04124088

Submitted on 9 Jun 2023

Mode of action of the natural herbicide radulanin A as an inhibitor of photosystem II.

Running title: Mode of action of radulanin A phytotoxicity

Simon THUILLIER[1,2], Stefania VIOLA[3,#], Bruce LOCKETT-WALTERS[2], Bastien NAY[2], Benjamin BAILLEUL[4] and Emmanuel BAUDOUIN[1,*]

[1]Laboratoire de Biologie du Développement, Institut de Biologie Paris Seine, Sorbonne Université, CNRS, Paris 75005, France

[2]Laboratoire de Synthèse Organique, Ecole Polytechnique, CNRS, Institut Polytechnique de Paris, Palaiseau 91128, France

[3]Department of Life Sciences, Imperial College – South Kensington Campus, London, UK

[4]Chloroplast Biology and Light-sensing in Microalgae-UMR7141, IBPC, CNRS-Sorbonne Université, Paris, France

[#]Current address : Photosynthesis & Environment team, Institut de Biosciences & Biotechnologies d'Aix-Marseille-UMR7265, CEA Cadarache, Saint-Paul-Lez-Durance 13115, France

Simon Thuillier (simon.thuillier@sorbonne-universite.fr)
Stefania Viola (stefania.viola@cea.fr)
Bruce Lockett-Walters (brucewalters74@gmail.com)
Bastien Nay (bastien.nay@polytechnique.edu)
Benjamin Bailleul (bailleul@ibpc.fr)
Emmanuel Baudouin (emmanuel.baudouin@sorbonne-universite.fr)

[*]Corresponding author :

Emmanuel Baudouin
Sorbonne Université, Institut de Biologie Paris-Seine (IBPS)
Laboratoire de Biologie du Développement, UMR CNRS 75622
Bâtiment C/2, boite courrier 24
9 quai St Bernard
75252 PARIS cédex 05 -France-

Email : emmanuel.baudouin@sorbonne-universite.fr
Tel : (+33) 1-44-27-59-87

Abstract

BACKGROUND

Radulanin A is a natural 2,5-dihydrobenzoxepin synthesized by several liverworts of the *Radula* genus. Breakthroughs in the total synthesis of radulanin A paved the way to the discovery of its phytotoxic activity. Nevertheless, its mode of action remained so far unknown and was investigated in *Arabidopsis thaliana*.

RESULTS

Radulanin A phytotoxicity was associated with cell death and partially depended on light exposure. Photosynthesis measurements based on chlorophyll *a* fluorescence evidenced that radulanin A and a Radula chromene inhibited photosynthetic electron transport with IC_{50} of 95 µM and 100 µM, respectively. We established a strong correlation between inhibition of photosynthesis and phytotoxicity for a range of radulanin A analogs. Based on these data, we also determined that radulanin A phytotoxicity was abolished when the hydroxyl group was modified and was modulated by the presence of the heterocycle and its aliphatic chain. Thermoluminescence studies highlighted that radulanin A targeted the Q_B site of the Photosystem II with a similar mode of action as 3-(3,4-dichloropheny)-1,1-dimethylurea (DCMU).

CONCLUSION

We establish that radulanin A targets Photosystem II, expanding Q_B sites inhibitors to bibenzyl compounds. The identification of an easy-to-synthesize analog of radulanin A with similar MoA and efficiency might be useful for future herbicide development.

Keywords : Radulanin A ; dihydrooxepines ; photosynthesis ; *Arabidopsis thaliana* ; Photosystem II ; Q_B site

1 INTRODUCTION

Weed management is a major issue for agriculture and essentially relies on the use of synthetic herbicides that represent more than half of the pesticide quantities sold annually.[1] Among synthetic herbicides, glyphosate holds a highly dominant position because of its broad-spectrum efficacy, relatively low cost, and the introduction of glyphosate-resistant crops in the 1990s. Herbicides cause severe damages to plant organs, possibly leading to the death of the entire plant. They differ in their phytotoxic dose range and host spectra, which can reflect a variety of modes of penetration and modes of action (MoA).[2] Nevertheless, the synthetic herbicides currently used target a limited array of metabolic pathways including photosynthesis, protein and lipid synthesis or cell wall formation, thereby favoring the selection of resistant weeds and jeopardizing weed management ([2] and references therein). The emergence of extensive herbicide resistance, together with the strengthening of environmental and health policies that restrict the use of synthetic herbicides, have raised new challenges and renewed interest in the search for new and environmentally-safer molecules.[3] In this context, natural products represent a wide source of bioactive molecules still under-utilized as herbicides. Interestingly, natural compounds structures generally lack halogen atoms or 'unnatural' rings, which could reduce their environmental impact by limiting their effective duration in the field compared to synthetic herbicides.[4]

The bryophyte lineage, that includes liverworts, hornworts and mosses, gathers the closest living relatives of the ancestral land plant species.[5] It rapidly diverged from the tracheophyte lineage and may therefore have retained ancestral traits present in land plant ancestors and lost in tracheophytes. Interestingly, bryophytes exhibit a remarkable and

3

specific chemical diversity that has been poorly studied.[6] Nevertheless, more than 2,000 secondary metabolites have been characterized in bryophytes, including a variety of terpenoids, flavonoids and lipids.[7] Among bryophytes, liverworts present the largest repertoire of natural products. In particular, they synthesize a huge diversity of bibenzyl-related compounds that has been recently reviewed in *Marchantiophyta* and in *Radula* genera.[8,9] Although their bioactivity is generally unknown, several bibenzyl-related compounds such as marchantins and perrottetins, exhibit antifungal, antimicrobial, anti-trypanosomal, and/or anti-viral activities and affect a large range of physiological and biochemical processes.[9] Beside these rare reports, no information is available on their possible phytotoxicity and potential as herbicide.

Radulanin A, 3-methyl-8-(2-phenylethyl)-2,5-dihydro-1-benzoxepin-6-ol, belongs to the 2,5-dihydrobenzoxepin group of bibenzyl compounds and has been isolated from liverworts of the *Radula* genus.[8] Scarce information on the bioactivity of radulanin A and its relatives, e.g. radulanin H and L, include the inhibition of calmodulin and lipoxygenase activities and the inhibition of nitric oxide production in lipopolysaccharide-treated macrophages.[10,11]Recently, together with the development of a new and simpler total synthesis of radulanin A, its phytotoxicity to the model plant *Arabidopsis thaliana* was described.[12,13]

In the present study, radulanin A phytotoxicity and MoA were further investigated using radulanin A analogs and synthetic intermediates. We report that radulanin A and a Radula chromene [10] which is also a synthetic precursor of radulanin A, impair Arabidopsis photosynthetic activity and thereby trigger plant death. Both compounds target photosystem

II (PSII) at the Q_B site and therefore expend the structural diversity of herbicidal Q_B site inhibitors. We also report the requirement of the phenol group for chromene bioactivity.

2 MATERIALS AND METHODS

2.1 Culture and treatment of *Arabidopsis thaliana* seedlings

Seeds of *Arabidopsis thaliana* ecotype Columbia-0 (Col-0) were surface-sterilized as previously described.[14] Fifteen seeds were sown per well in sterile 96-well plates in the presence of 150 μL of sterile distilled water and stratified for 3 days at 4 °C. Plates were then transferred in a growth chamber at 21°C, under continuous light (40 μmol photons m^{-2} s^{-1}). After 9-13 days, water was removed and replaced by 200 μL of sterile distilled water supplemented with the proper concentrations of tested chemicals, that we prepared through known procedure [12] by the condensation of dihydropinosylvin and appropriate aldehydes (for full description, refer to Supplementary Material). Stock solutions (40 mM in DMSO) were stored at -20 °C and diluted extemporaneously in water (35-400 μM final) for plantlet treatment. For all conditions, the final concentration of DMSO represented ≤1 % of the total volume used for treatment. Bromoxynil and 3-(3,4-dichloropheny)-1,1-dimethylurea (DCMU) were purchased from Sigma-Aldrich (Lyon, France). Stocks solutions (100 mM for bromoxynil and 10 mM for DCMU in ethanol) were diluted extemporaneously before treatment in water (100 μM and 10 μM final, respectively). In all experiments, plantlets treated with 1% DMSO were used as controls.

2.2 Chlorophyll fluorescence measurements

Chlorophyll fluorescence measurements were performed on seedlings (10-15 per well) in a 96-well plate at room temperature using a fluorescence imaging setup (Speedzen, JBeamBio,

France). Samples were dark adapted for 10 min prior to analysis. Green LEDs provided actinic light at 120 μmol photons m^{-2} s^{-1} and saturating pulses at 2600 μmol photons m^{-2} s^{-1}. Measurement pulses were provided by blue LEDs. Maximal quantum efficiency of PSII was calculated as $F_v/F_m = (F_m - F_o)/F_m$, where F_o and F_m are the fluorescence emission measured before and at the end of a 200 ms saturating pulse, respectively, in dark adapted leaves. Φ_{PSII} was calculated as $(F_m'-F)/F_m'$, with F being the steady-state fluorescence reached in presence of illumination with actinic light and F_m' being the fluorescence emission measured at the end of a 200 ms saturating pulse, in the light-adapted leaves. Non photochemical quenching (NPQ) was calculated as $(F_m-F_m')/F_m'$.[15] Data were obtained from two independent experiments gathering 6 biological samples (60-90 plantlets).

2.3 P700 redox state measurements

P700 redox state was measured at room temperature through transient absorption changes by a Joliot-type spectrophotometer (JTS-10, Biologic, Grenoble, France). The absorption changes were measured at 705 ± 6 nm. The actinic light was provided by a crown of red LEDs (λ = 619 nm) at 26 μmol photons m^{-2} s^{-1}, that also provided the 20 ms saturating light pulses at 5000 μmol photons m^{-2} s^{-1}. Seedlings from 4 wells treated separately were pooled to cover the light path for each replicate. Data from each condition represent the mean ± S.D from 3 independent biological replicates.

2.4 Thermoluminescence

Thermoluminescence curves were measured with a laboratory-built apparatus, described in De Causmaecker et al. (https://spiral.imperial.ac.uk/handle/10044/68272). Samples were cooled to -20 °C and excited with a single turnover saturating laser flash (Continuum Minilite

II, frequency doubled to 532 nm, 5 ns FWHM). The samples were then incubated in the dark at -20 °C for 30 s, before heating from -20 °C to 80 °C at 1 °C s^{-1}. When used, Arabidopsis seedlings immersed in water were incubated in the dark at room temperature in presence of 400 µM radulanin A, 10 µM DCMU or 100 µM bromoxynil for the indicated amount of time before the measurements. PSII-enriched membrane fragments from spinach, prepared according to Berthold et al.[16] were diluted to a final chlorophyll concentration of 10 µg mL^{-1} in ice-cold resuspension buffer (50 mM MES-NaOH pH 6.5, 5 mM CaCl$_2$, 10 mM MgCl$_2$, 1.2 M betaine, 20 % w/v glycerol). The samples were pre-illuminated with room light for 10 s and then kept in the dark on ice for at least 1 hour before measurement. When tested, 400 µM radulanin A, 10 µM DCMU or 100 µM bromoxynil were added to the dark-adapted samples either right before measurement or for a specific incubation time. As controls, thermoluminescence curves were measured using plantlets or membrane fragments treated with 1% DMSO.

2.5 Statistical analysis

Results are represented as mean ± standard deviation (SD). Differences between control condition and other treatments were analyzed with GraphPad Prism 6.0 software (GraphPad Software Inc., San Diego USA) using One-Way ANOVA followed by post-hoc Dunn's test.

3 RESULTS

3.1 Radulanin A and its precursors and structural analogs present different level of phytotoxicity on Arabidopsis.

As previously reported, radulanin A exhibited a phytotoxic effect on *Arabidopsis thaliana* (Arabidopsis in the following) seedlings.[13] To obtain insights into the structures required for radulanin A biological activity, we compared its toxicity to that of its synthetic precursors and several structural analogs that we synthesized according to the procedure described in Supplementary material and in Lockett-Walters et al.[12] Thus, the phytotoxicity of these 13 structural analogs of radulanin A was compared using chlorosis as a proxy for plantlet death (Fig. 1). As reported previously [13], chlorosis was observed upon radulanin A (**4**) treatment. Chlorosis was obvious after 7 days of treatment and for doses above 100 µM (Fig. 1). Radulanin A cyclic analogs and their saturated versions (compounds **3, 5, 7,** and **8**) had a similar efficiency. In contrast, dihydropinosylvin (**2**) and chromene **11** was slightly less active, with a minimum concentration of 150 µM required to induce chlorosis. This lower activity was more obvious with chromene **9** and chromene **12**, for which only the higher dose tested induced bleaching. Finally, *O*-methylated dihydropinosylvin (**1**), *O*-substituted compounds (**6** and **10**), and chromene **14** were not phytotoxic. The same effects were observed when the death of seedlings was directly analyzed using Trypan blue staining, indicating that the effect of radulanin A and its bioactive analogs led to cell death (Fig. S1). As a whole, these data indicate that the bioactivity of radulanin A requires the presence of its hydroxyl group and is modulated by the presence of the heterocycle and its aliphatic chain.

3.2 Radulanin A and several analogs impair photosynthesis.

When radulanin A treatments were carried out in darkness, no chlorotic phenotype was observed, indicating that light was required for phytotoxicity (Fig. S2). We therefore postulated that photosynthesis was likely targeted by radulanin A and its analogs. To assess

their impact on photosynthesis, we first treated plants for 12 h and then used chlorophyll *a* fluorescence to probe PSII activity (Fig. 2). We measured the maximal quantum yield of PSII and its quantum yield under illumination (F_v/F_m and Φ_{PSII} respectively, see Material and Methods). F_v/F_m is measured in dark-adapted plants, and represents the maximum capacity of PSII for photochemistry. The F_v/F_m of control seedlings was 0.79 ± 0.01, a typical value for healthy plants (Fig. 2A), and was not statistically altered in the presence of 1% DMSO (Fig. S3). It indicates that approximately 79 % of the photons absorbed by the PSII end up being converted into a photochemical event when the PSII is not constrained by downstream reactions. Treatments with radulanin A or Radula chromene **3** resulted in a dose-dependent decrease in F_v/F_m in a concentration range of 35-400 μM, indicating that the integrity/photochemical capacity of PSII is impaired (IC_{50} are 95 μM and 100 μM for radulanin A and Radula chromene **3**, respectively; Table 1). The quantum yield of PSII was also measured under a 10 min green illumination (120 μmol photons m^{-2} s^{-1}, see Material and Methods). Once steady state photosynthesis is achieved, Φ_{PSII} does not only depend on the intrinsic photochemical capacity of PSII but also on the rate-limiting step of the photosynthetic electron transfer chain (ETC) downstream of it, because of the serial work of photosynthetic complexes. Similarly to F_v/F_m, Φ_{PSII} was inhibited by both molecules in the same concentration range and with a comparable calculated IC_{50} (89 μM and 101 μM for radulanin A and Radula chromene **3**, respectively) (Fig. 2B and Table 1).

The effect of the different analogs on Φ_{PSII} was compared after 12h of treatment at 400 μM (Fig. 2C). Compared to DMSO treatment, radulanin A and all compounds inducing seedling chlorosis (Fig. 1) inhibited Φ_{PSII}. The Φ_{PSII} inhibition was less pronounced for chromene **9** and **12,** in agreement with their lower phytotoxicity and was absent for compounds that did not induce chlorosis, such as *O*-methylated compounds (**1** and **6**) and chromene **14**. At a lower

9

dose (100 µM), only radulanin A, Radula chromene (**3**), tylimanthin B (**5**) and chromane (**7**) statistically inhibited Φ_{PSII} (Fig. 2D). Together, these data indicate a strong correlation between ETC inhibition and chlorosis-based phytotoxicity assessment, suggesting that the primary target of the herbicide radulanin A is photosynthetic ETC.

To clarify the primary target of radulanin A in photosynthetic ETC, we followed the kinetics of F_v/F_m and Φ_{PSII} as a function of treatment duration (Fig. 3A and 3B). The magnitude and kinetics of the F_v/F_m decrease depended on the concentration of radulanin A. The final F_v/F_m values after 12 h of treatment were 0.49 ± 0.14, 0.20 ± 0.10 and 0.12 ± 0.09 for 100, 150 and 400 µM of radulanin A, respectively. In water without any addition or in the presence of 1% DMSO (Fig. S3A), the F_v/F_m remained constant throughout the experiment (0.80 ± 0.01). The rate of decline in F_v/F_m over time was also correlated with radulanin A concentration: Fv/Fm values reached steady state after approximately 8 h with 400 µM but still decreased after 12 h with 100 µM radulanin A (Fig. 3A). Φ_{PSII} decreased over time for all radulanin A concentrations and reached a plateau after 5 to 10 h (Fig. 3B). No effect was observed in the presence of 1 % DMSO compared to water conditions, with values of 0.59-0.6 throughout the experiment (Fig. S3B). After 12 h of treatment, Φ_{PSII} was 0.28 ± 0.13, 0.13 ± 0.08 and 0.07 ± 0.08 at 100 µM, 150 µM and 400 µM radulanin A, respectively. The inhibition of the photosynthetic electron transfer also resulted in a decrease of Non-Photochemical Quenching (NPQ) (Fig. 3C). The fast fluorescence rise at the dark-to-light transition (which is similar to the OJ part of the OJIP curves, see (Stirbet and Govindjee, 2011)) displays a higher magnitude after 15 minutes of 400 µM radulanin A treatment, compared to the control (Fig. 3D).

Similar magnitudes and kinetics of F_v/F_m and Φ_{PSII} inhibition were measured for Radula chromene (**3**) and similar effects were also observed on NPQ or fluorescence increase at the light onset (Fig. S4). Interestingly, after 15 min of treatment, Φ_{PSII} was reduced under radulanin

A or Radula chromene treatment when F_v/F_m remained unchanged (Fig. 3A and 3B, Fig. S4A and S4B). The fact that the decrease of Φ_{PSII} preceded that of F_v/F_m indicates that the initial target of radulanin A is not the photochemistry of PSII *per se* but another step of the ETC and that the degradation of the integrity/photochemical capacity of PSII comes later or is an indirect consequence of inhibition of this step of ETC.

3.3 The site of action of radulanin A is located in the inter-system chain.

Since radulanin A and its structural analogs inhibit photosynthetic ETC, we wanted to localize more precisely the site of inhibition and wondered whether the inhibition was downstream or upstream of Photosystem I (PSI). For this, we investigated the redox state of P700, the chlorophyll PSI, during continuous illumination under treatments of different durations with radulanin A or analogs (Fig. 4). Under control conditions, Arabidopsis seedlings have 47 ± 3 % of P700 oxidized (compared to the maximum of photo-oxidizable P700) under illumination conditions (see Material and Methods). A similar value (46 ± 2 %) was obtained after treatment with the hitherto ineffective *O*-methylated chromene **6** at 400 µM (Fig 4A and 4B). As expected, 3-(3,4-dichlorophenyl)-1,1-dimethylurea (DCMU), a well-known and effective PSII inhibitor (used at 10 µM), led to an accumulation of 97 ± 1 % of P700$^+$. Radulanin A and chromene **3** (both used at a concentration of 400 µM) induced the accumulation of 69 ± 4 % and 72 ± 5 % of P700$^+$, respectively. The higher oxidation of P700 after treatment with radulanin A and chromene **3** implies that the site of inhibition is located upstream of PSI photochemistry in the ETC. Together with the higher amplitude of the OJ phase at the light onset in the presence of radulanin A and its analogs, this pinpoints the site of inhibition between PSII and PSI photochemical events, *i.e*. in the inter-system chain. Such phenotypes are characteristic of PSII Q_B site inhibitors such as DCMU and prompted us to test the

hypothesis that radulanin A and its analogs target the Q_B site of PSII with thermoluminescence (TL) [17].

3.4 Radulanin A and chromene 3 are Q_B site inhibitors.

PSII-enriched membrane fragments from spinach were employed to study the effect of radulanin A and two structural analogs, Radula chromene **3** and its *O*-methylated analog **6,** as well as two control Q_B site inhibitors, bromoxynil and DCMU [18] on thermoluminescence curves (Fig. 5A and 5B). All compounds were applied at 400 µM, except bromoxynil and DCMU which were used at 100 µM and 10 µM respectively, as previously described [19,20]. In DMSO-treated control samples, maximum thermoluminescence was observed at 44°C (Fig. 5). Such temperature which corresponds to T_{max} is typical for the $S_2Q_B^-$ recombination [17]. Treatments with DCMU and bromoxynil led to a shift of T_{max} towards 16 °C and 4°C, respectively (Fig. 5A). Such change in T_{max} values reflects a recombination of the $S_2Q_A^-$ state, where the electron is blocked at the Q_A site [17,18]. In the presence of radulanin A, maximum thermoluminescence was reached for a T_{max} of 14 °C, similar to that of DCMU (Fig. 5A). The thermoluminescence curve measured in the presence of Radula chromene **3** overlapped that of radulanin A, with a similar T_{max} of 15 °C (Fig. 5B). In contrast, application of *O*-methylated chromene **6** did not modify the T_{max} (41°C) measured under control conditions. As observed in Fig. 5C, the effect of radulanin A on T_{max} shift depended on the concentration applied. Indeed, T_{max} decreased to 33°C, 19°C and 15°C when 50 µM, 200 µM and 400 µM of radulanin A were applied, respectively. Finally, to examine the kinetics of radulanin effect on T_{max}, thermoluminescence curves were acquired after different duration of treatment (Fig 5D). The effect of radulanin A addition on the Tmax shift was immediate, and no further changes in the TL peak were observed during further 6 h

of treatment. As a whole, these results indicated that radulanin A and Radula chromene **3** function as Q_B inhibitors.

To further address the effect of radulanin A *in planta*, thermoluminescence measurements were also performed on Arabidopsis seedlings (Fig. 6). In DMSO-treated plantlets thermoluminescence arising from $S_2Q_B^-$ recombination was observed, having a T_{max} of 40-50 °C. As observed in PSII-enriched membrane fragments, a shift of the T_{max} (to 0.5°C, in seedlings) was observed 6h after radulanin A treatment (Fig. 6A and 6B). Interestingly, this shift occurred progressively (Fig. S5), in contrast to experiments performed on PSII-enriched membrane fragments where changes were immediate (Fig. 5D). Compared to radulanin A, DCMU and bromoxynil treatments led to similar changes in T_{max} (Fig. 6A). As observed in Fig. 5B, application of chromene **3** to plantlets mimicked the effect of radulanin A, when its O-methylated analog did not modify T_{max} significantly (Fig. 6B). Radulanin A and Radula chromene **3** therefore appear as potent Q_B site inhibitors *in planta*.

4 DISCUSSION

Radulanin A is a 2,5-dihydrobenzoxepin found in numerous liverworts of the *Radula* genus that exhibits phytotoxicity towards *Arabidopsis thaliana* [13]. In the present study, we evidenced that the herbicide activity of radulanin A involves the inhibition of photosynthetic electron transport and requires specific structural features shared by some of its bioactive precursors and analogs. Through our investigation, chlorosis and permanent damage were correlated with the inhibition of photosynthesis. Chlorophyll *a* fluorescence brought a first insight in the alteration of the photosynthetic ETC after treatment. Since short treatment

13

times induced a decrease of ϕ_{PSII} but not of Fv/Fm, it was concluded that the studied phytotoxic compounds did not inhibit the capacity of PSII to perform photochemistry.

Most of the herbicides, but also structurally-unrelated natural products, affecting the photosynthetic ETC specifically target the Q_B site of PSII, mainly formed by its D1 protein subunit [21–26]. Others, such as diquat or paraquat, divert photosynthetic electrons downstream PSI [27,28]. The higher oxidation of P700 during illumination induced by radulanin A indicated that the site of inhibition is located upstream of PSI. As we evidenced by thermoluminescence studies performed on PSII-enriched membrane fragments, radulanin A and chromene **3** function as photosynthesis inhibitors by binding to the Q_B site. Indeed, treatments with either compound led to TL curves and T_{max} similar to those observed after treatment with the Q_B site inhibitor DCMU, but higher than those observed in presence of the herbicide bromoxynil, another well-known Q_B site inhibitor. Such differences in thermoluminescence curves have been previously reported for bromoxynil and DCMU and serve for herbicide classification [18]. Interestingly, contrarily to PSII-enriched membrane fragments, TL ratio between 0.5 °C and 50 °C was modified in radulanin A-treated seedling in a time-dependent manner. This variation illustrates a progressive increase of Q_A^- and decrease of Q_B^- [17] which was not observed in PSII-enriched membrane fragments where only $S_2Q_A^-$ recombination TL peak is present right after the addition of the inhibitor. While the binding of the inhibitor to the Q_B site is instantaneous as observed for PSII-enriched membrane fragments, such delay in intact seedlings reflects the time-dependent diffusion towards the site of action. Moreover, DCMU-treated seedlings displayed a low TL at 50 °C while TL at 0 °C was very intense, in contrast to radulanin A treatment. This difference implies that more Q_B sites are occupied by DCMU than by radulanin A after 5 h of treatment and suggests that radulanin A binds to the Q_B site less efficiently than DCMU. Because comparable TL curves and T_{max} are observed for radulanin A and DCMU

treatments, it is likely that radulanin A (and Radula chromene **3**) binds to Q_B site in a similar way to DCMU, possibly *via* a hydrogen bond to D1-Ser264 as reported for DCMU [29]. In contrast, radulanin A binding to Q_B site differs from bromoxynil binding, although both molecules share a phenol group that is absent in DCMU and is important for bromoxynil binding [29]. Docking studies evidenced that bromoxynil binding within Q_B site depends on the protonation of the phenol group. Indeed, protonated bromoxynil docks in the Q_B site by interacting with D1-Phe265/Ser264 whereas its deprotonated form binds to D1-His215 [29]. *In vivo*, bromoxynil scarcely binds to D1-Phe265/Ser264 because the low pKa (4.2) of its phenol group [30] compared to stromal pH (7-8) [31] makes the phenol group mostly deprotonated. This behavior can be extrapolated to our experimental setup in which pH was maintained to 6.5. In these conditions, based on its chemical environment, the phenol group of radulanin A is expected to be essentially protonated within the Q_B site due to a pKa (~9.5) higher than external pH, which could account for the differences observed between radulanin A and bromoxynil. Docking studies are now required to further investigate these hypotheses and to determine if radulanin A docking only involves a hydrogen bond with D1-Ser264 or involves additional bonds, as reported for a range of natural herbicides. Compared to other natural Q_B site inhibitors *e.g.* stigmatellin[32], sorgoleone[23], fischerellin[33] or patulin[22] and with the exception of gliotoxin[34] and tenuazonic acid[35], radulanin A presents a high I_{50} for ϕ_{PSII}, suggesting it is a rather weak inhibitor of PSII. Therfore, beside its action at Q_B site, it cannot be ruled out that radulanin A also impacts the function of additional targets, as has been observed for other natural inhibitors of the Q_B site. For instance, stigmatellin from the myxobacterium *Stigmatella aurantiaca* not only targets the Q_B site but also inhibits the cytochrome *b₆f* complex [32].

The identification of radulanin A as a potent photosynthesis inhibitor made it possible to investigate the structural requirements for radulanin A bioactivity. To address this issue, we synthesized radulanin A precursors and analogs [12] and tested their inhibitory effect on ETC. Interestingly, seven of the compounds (**1**, **2**, **3**, **4**, **5**, **6** and **14**) tested in these experiments are also naturally found in Radula species [8] and in a variety of other plant species in the case of **1** and **2** [36–42]. On the one hand, the absence or substitution of the phenol group abolished ETC inhibition. To a lesser extent, the absence of the phenylethyl chain and the elongation of the lipophilic chain of the heterocycle, also reduced inhibition, that was only observed for the highest doses tested. The cyclic analogs and their hydrogenated versions, instead, showed a similar inhibition efficiency as radulanin A. Strikingly, the efficiency of radulanin A analogs to inhibit photosynthetic ETC fully correlated with their ability to trigger plant death, indicating that the inhibition of photosynthetic ETC activity is an essential aspect of their phytotoxicity. Moreover, the comparison of the modes of action of radulanin A and Radula chromene **3** highlighted that both molecules impair ETC through the inhibition of Q_B site. In the same experiments, *O*-methylated chromene did not inhibit ETC and did not bind Q_B site. It is therefore likely that the biologically-active radulanin A analogs, *i.e.* based on a phenolic bibenzyl backbone, share the same MoA. Beside those tested, numerous radulanin A analogs have been identified in Radula species [8] that could be screened for ETC inhibition to further investigate the structural bases of radulanin A bioactivity. Furthermore, several natural products from the orchid *Epidendrum rigidum* reported as phytotoxic also share a phenolic bibenzyl backbone, suggesting that the relationship between structure and function highlighted in our study could be extended to other natural analogs [43]. Noteworthy, two of these bibenzyl compounds, batatasin III and gigantol, also share anti-calmodulin activity with

radulanin A, which strengthens the hypothesis of common structurally-based functionalities [44,45].

5 Conclusions

Radulanin A has been the first compound from liverworts reported for its herbicide activity [13]. In this study, we further unraveled the MoA of this compound that makes it the only 2,5-dihydrobenzoxepin, and more generally bibenzyl, characterized so far as a potent Q_B site inhibitor. Because of the conservation of Q_B site structure and function among plants, radulanin A could be phytotoxic towards a large range of weeds. Its chemical structure and liverwort origin makes it also an original compound for the development of new herbicides. Although radulanin A appears as a rather weak PSII inhibitor, its herbicidal efficiency can be greatly improved by the structure-based design of new analogs as performed with other natural herbicides [46]. Beside the herbicidal efficiency, the availability of large amounts of active principle is crucial for herbicide development. Even though we improved the simplicity and yield of production by recently establishing a new synthesis [12], the total synthesis of radulanin A remains challenging and a bottleneck for future developments. In this respect, our study suggests that Radula chromene **3**, that is also a natural product [10] and a synthetic precursor of radulanin A, is a valuable alternative, as it presents similar I_{50} and MoA and can be synthesized more easily than radulanin A [12].

Conflict of Interest Declaration

Authors declare no conflicts of interest.

References

1 Qu RY, He B, Yang JF, Lin HY, Yang WC, Wu QY, *et al.*, Where are the new herbicides?, *Pest Manag Sci* **77**:2620-2625 (2021).

2 Dayan FE, Current status and future prospects in herbicide discovery, *Plants* **8** (2019).

3 Sparks TC and Bryant RJ, Crop protection compounds – trends and perspective, *Pest Manag Sci* **77**:3608–3616 (2021).

4 Soltys D, Krasuska U, Bogatek R, Gniazdowska A, Soltys D, Krasuska U, *et al.*, Allelochemicals as bioherbicides — present and perspectives, *Herbic - Curr Res Case Stud Use*, IntechOpen (2013).

5 Wang Q-H, Zhang J, Liu Y, Jia Y, Jiao Y-N, Xu B, *et al.*, Diversity, phylogeny, and adaptation of bryophytes: insights from genomic and transcriptomic data, *J Exp Bot* **73**:4306–4322 (2022).

6 Horn A, Pascal A, Lončarević I, Volpatto Marques R, Lu Y, Miguel S, *et al.*, Natural products from bryophytes: from basic biology to biotechnological applications, *Crit Rev Plant Sci* **40**:191–217 (2021).

7 Sabovljević MS, Sabovljević AD, Ikram NKK, Peramuna A, Bae H, and Simonsen HT, Bryophytes – an emerging source for herbal remedies and chemical production, *Plant Genet Resour* **14**:314–327 (2016).

8 Asakawa Y, Nagashima F, and Ludwiczuk A, Distribution of bibenzyls, prenyl bibenzyls, bis-bibenzyls, and terpenoids in the liverwort genus *Radula*, *J Nat Prod* **83**:756–769 (2020).

9 Asakawa Y, Ludwiczuk A, Novakovic M, Bukvicki D, and Anchang KY, Bis-bibenzyls, bibenzyls, and terpenoids in 33 genera of the *Marchantiophyta* (liverworts): structures,

synthesis, and bioactivity, *J Nat Prod* **85**:729–762 (2022).

10   Asakawa Y, Hashimoto T, Takikawa K, Tori M, and Ogawa S, Prenyl bibenzyls from the liverworts *Radula perrottetii* and *Radula complanata*, *Phytochemistry* **30**:235–251 (1991).

11   Harinantenaina L, Takahara Y, Nishizawa T, Kohchi C, Soma GI, and Asakawa Y, Chemical constituents of malagasy liverworts, part V: prenyl bibenzyls and clerodane diterpenoids with nitric oxide inhibitory activity from *Radula appressa* and *Thysananthus spathulistipus*, *Chem Pharm Bull* **54**:1046–1049 (2006).

12   Lockett-Walters B, Thuillier S, Baudouin E, and Nay B, Total synthesis of phytotoxic Radulanin A facilitated by the photochemical ring expansion of a 2,2-dimethylchromene in flow, *Org Lett* **24**:4029–4033 (2022).

13   Zhang W, Baudouin E, Cordier M, Frison G, and Nay B, One-pot synthesis of metastable 2,5-dihydrooxepines through retro-Claisen rearrangements: method and applications, *Chem – Eur J* **25**:8643–8648 (2019).

14   Cantrel C, Vazquez T, Puyaubert J, Rezé N, Lesch M, Kaiser WM, *et al.*, Nitric oxide participates in cold-responsive phosphosphingolipid formation and gene expression in *Arabidopsis thaliana*, *New Phytol* **189**:415–427 (2011).

15   Maxwell K and Johnson GN, Chlorophyll fluorescence—a practical guide, *J Exp Bot* **51**:659–668 (2000).

16   Berthold DA, Babcock GT, and Yocum CF, A highly resolved, oxygen-evolving photosystem II preparation from spinach thylakoid membranes, *FEBS Lett* **134**:231–234 (1981).

17   Ducruet J-M and Vass I, Thermoluminescence: experimental, *Photosynth Res* **101**:195–204 (2009).

18   Vass I and Demeter S, Classification of photosystem II inhibitors by thermodynamic characterization of the thermoluminescence of inhibitor-treated chloroplasts, *Biochim Biophys Acta* **682**:496–499 (1982).

19   Ahmadova N, Ho FM, Styring S, and Mamedov F, Tyrozine D oxidation and redox equilibrium in photosystem II, *Biochim Biophys Acta* **1858**:407–417 (2017).

20   Fufezan C, Rutherford AW, and Krieger-Liszkay A, Singlet oxygen production in herbicide-treated photosystem II, *FEBS Lett* **532**:407–410 (2002).

21   Dayan FE and Duke SO, Natural compounds as next-generation herbicides, *Plant Physiol*

166:1090–1105 (2014).

22 Guo Y, Liu W, Wang H, Wang X, Qiang S, Kalaji HM, *et al.*, Action mode of the mycotoxin patulin as a novel natural photosystem II inhibitor, *J Agric Food Chem* **69**:7313–7323 (2021).

23 Czarnota MA, Paul RN, Dayan FE, Nimbal CI, and Weston LA, Mode of action, localization of production, chemical Nature, and activity of sorgoleone: a potent PSII inhibitor in Sorghum spp. root exudates, *Weed Technol* **15**:813–825 (2001).

24 Spyridaki A, Fritzsch G, Kouimtzoglou E, Baciou L, and Ghanotakis D, The natural product capsaicin inhibits photosynthetic electron transport at the reducing side of photosystem II and purple bacterial reaction center: structural details of capsaicin binding, *Biochim Biophys Acta* **1459**:69–76 (2000).

25 Nain-Perez A, Barbosa LCA, Maltha CRA, Giberti S, and Forlani G, Tailoring natural abenquines to Inhibit the photosynthetic electron transport through interaction with the D1 protein in photosystem II, *J Agric Food Chem* **65**:11304–11311 (2017).

26 Chen S, Kim C, Lee JM, Lee H-A, Fei Z, Wang L, *et al.*, Blocking the QB-binding site of photosystem II by tenuazonic acid, a non-host-specific toxin of Alternaria alternata, activates singlet oxygen-mediated and EXECUTER-dependent signalling in Arabidopsis, *Plant Cell Environ* **38**:1069–1080 (2015).

27 Herbicide Resistance Action Committee (HRAC), HRAC Mode of Action Classification 2022.

28 Preston C, Resistance to photosystem I disrupting herbicides, *in* Herbicide resistance in plants, ed. by Powles SB, CRC Press, Boca Raton, pp 61-82 (1994).

29 Takahashi R, Hasegawa K, Takano A, and Noguchi T, Structures and binding sites of phenolic herbicides in the QB pocket of photosystem II, *Biochemistry* **49**:5445–5454 (2010).

30 Cessna AJ and Grover R, Spectrophotometric determination of dissociation constants of selected acidic herbicides, *J Agric Food Chem USA* **26**:289-292 (1978).

31 Kramer DM, Sacksteder CA, and Cruz JA, How acidic is the lumen?, *Photosynth Res* **60**:151–163 (1999).

32 Oettmeier W, Godde D, Kunze B, and Höfle G, Stigmatellin. A dual type inhibitor of photosynthetic electron transport, *Biochim Biophys Acta* **807**:216–219 (1985).

33 Srivastava A, Jüttner F, and Strasser RJ, Action of the allelochemical, fischerellin A, on

photosystem II, *Biochim Biophys Acta* **1364**:326–336 (1998).

34   Guo Y, Cheng J, Lu Y, Wang H, Gao Y, Shi J, *et al.*, Novel action targets of natural product gliotoxin in photosynthetic apparatus, *Front Plant Sci* **10** (2020).

35   Chen S, Xu X, Dai X, Yang C, and Qiang S, Identification of tenuazonic acid as a novel type of natural photosystem II inhibitor binding in QB-site of *Chlamydomonas reinhardtii*, *Biochim Biophys Acta* **1767**:306–318 (2007).

36   Lindstedt G, Misiorny A, Rubin I, Saluste E, Stjernholm R, and Ehrensvärd G, Constituents of pine heartwood. XXV. Investigation of forty-eight pinus species by paper partition chromatography., *Acta Chem Scand* **5**:121–128 (1951).

37   Fagboun D, Ogundana S, Adesanya SA, and Roberts M, Dihydrostilbene phytoalexins from *Dioscorea rotundata*, *Phytochemistry* **26**:3187–3189 (1987).

38   Fang JM, Su W-C, and Cheng YS, Flavonoids and stilbenes from armand pine, *Phytochemistry* **27**:1395–1397 (1988).

39   Kaganda NG and Adesanya SA, A new dihydrostilbene from diseased *Dioscorea mangenotiana*, *J Nat Prod* **53**:1345–1346 (1990).

40   Yamaki M, Kato T, Bai L, Inoue K, and Takagi S, Methylated stilbenoids from *Bletilla striata*, *Phytochemistry* **30**:2759–2760 (1991).

41   Kostecki K, Engelmeier D, Pacher T, Hofer O, Vajrodaya S, and Greger H, Dihydrophenanthrenes and other antifungal stilbenoids from *Stemona cf. pierrei*, *Phytochemistry* **65**:99–106 (2004).

42   Boonphong S, Puangsombat P, Baramee A, Mahidol C, Ruchirawat S, and Kittakoop P, Bioactive compounds from *Bauhinia purpurea* possessing antimalarial, antimycobacterial, antifungal, anti-inflammatory, and cytotoxic activities, *J Nat Prod* **70**:795–801 (2007).

43   Hernández-Romero Y, Acevedo L, de Los Ángeles Sánchez M, Shier WT, Abbas HK, and Mata R, Phytotoxic activity of bibenzyl derivatives from the orchid *Epidendrum rigidum*, *J Agric Food Chem* **53**:6276–6280 (2005).

44   Hernández-Romero Y, Rojas J-I, Castillo R, Rojas A, and Mata R, Spasmolytic effects, mode of action, and structure–activity relationships of stilbenoids from *Nidema boothii*, *J Nat Prod* **67**:160–167 (2004).

45   Asakawa Y, Biologically active compounds from bryophytes, *Pure Appl Chem* **79**:557–580 (2007).

46   Wang H, Yao Q, Guo Y, Zhang Q, Wang Z, Strasser RJ, *et al.*, Structure-based ligand design and discovery of novel tenuazonic acid derivatives with high herbicidal activity, *J Adv Res* **40**:29–44 (2022).

	Φ_{PSII}			F_V/F_M		
	IC$_{50}$ (μM)	95% CI	R^2	IC$_{50}$ (μM)	95% CI	R^2
Radula chromene (**3**)	101	85-109	0.90	100	85-106	0.92
Radulanin A (**4**)	89	80-102	0.92	95	84-105	0.93

Table 1 : IC50 of radulanin A and its chromene precursor regarding Φ_{PSII} and Fv/Fm parameters. IC50 was calculated upon data shown Figure 2A and 2B. 95% confidence interval (95% CI) is presented. R^2 was determined by non-linear fit regression.

Figure legends

Figure 1: Effect of radulanin A and its structural analogs on Arabidopsis seedling viability. Pictures were taken 1 week after treatment and are representative of 3 experiments. Control refers to 1% DMSO treatment. Dark squares indicate the minimal bioactive concentration for each molecule. Compounds are identified by their numbers in the text, together with current names for 2 (dihydropinosylvin), 3 (Radula chromene), 4 (radulanin A), 5 (tylimanthin B), 6 (O-methylated chromene) and 7 (chromane). The main compounds used in this study (**3**, **4** and **6**) are color-labeled and the color code is maintained across the different figures.

Figure 2: Effect of radulanin A and its analogs on PSII maximal efficiency (Fv/Fm) and PSII quantum yield activity (Φ_{PSII}). Fv/Fm **(A)** and Φ_{PSII} **(B)** were measured on Arabidopsis seedlings after 12 h of treatment with different concentrations of radulanin A (orange circles) or Radula chromene **3** (green triangles). **C**, Φ_{PSII} was measured after 12 h of treatment with 400 μM of radulanin A or with its analogs. **D**, Φ_{PSII} was measured after 12 h of treatment with 100 μM of the molecules identified as bioactive in panel C. Control corresponds to treatment with 1% DMSO. Results are given as mean ± S.E (n=3-6). Asterisks indicate statistical differences between control and treatments as determined by One-Way ANOVA followed by post-hoc Dunn's test (** $P<0.01$, **** $P<10^{-4}$).

Figure 3: Evolution of PSII parameters after radulanin A treatment. Chlorophyll fluorescence measurements were performed on Arabidopsis seedlings treated with 1% DMSO (control) or different concentrations of radulanin A. **A**. PSII maximal efficiency (F_v/F_m), **B**. PSII quantum yield activity (Φ_{PSII}), **C**. Non-photochemical quenching (NPQ), **D**. Measured relative fluorescence. Represented data are the means ± SD of 6 independent biological replicates.

Figure 4: Effect of radulanin A on P700 redox activity. Transient absorption changes were measured at 705 nm for Arabidopsis seedlings treated with 1% DMSO (control), 10 μM DCMU or radulanin A and different structural analogs at 400 μM. The seedlings were harvested after 15 min of treatment and measurements were performed after 2 min under actinic light (26 μmol photons.m^{-2}.s^{-1}). **A**. The ΔI/I was measured during actinic illumination (negative time values) and during and after a saturating light pulse given at time point zero. The decay was

followed for 1565 ms in the dark after the pulse offset, before actinic light was switched on again. All the recorded traces were normalised on the difference between the ΔI/I recorded during actinic illumination and the one recorded at the end of the dark decay. **B**. Percentage of reduced P700 after 15 min of treatment. Represented data are the means ± SD of 3 independent biological replicates. Asterisks indicate statistical differences between control and treatments as determined by One-Way ANOVA followed by post-hoc Dunn's test (*** $P<0.001$, **** $P<10^{-4}$).

Figure 5: Thermoluminescence of treated PSII-enriched membrane fragments. Control refers to 1% DMSO treatment. Except in panel D, measurements were performed immediately after treatment. **A**. Effect of radulanin A (400 μM), and Q_B site inhibitors (DCMU 10 μM, bromoxynil 100 μM). **B**. Effect of radulanin A, Radula chromene **3** and its *O*-methylated analog (400 μM) on thermoluminescence., **C**. Dose-response study over radulanin A treatment, **D**. Effect of radulanin A (400 μM) treatment duration.

Figure 6: Thermoluminescence of Arabidopsis treated seedlings. Control refers to 1% DMSO treatment. Measurements were performed 6 h after treatment. **A**. Effect of radulanin A (400 μM), and Q_B site inhibitors (DCMU 10 μM, bromoxynil 100 μM). **B**. Effect of radulanin A, Radula chromene **3** and its *O*-methylated analog (400 μM) on thermoluminescence.
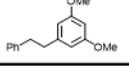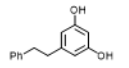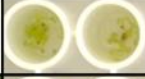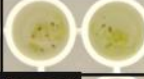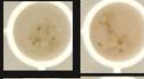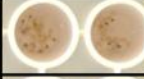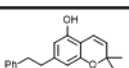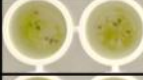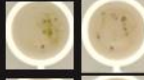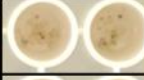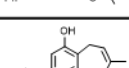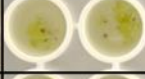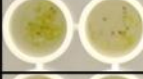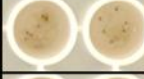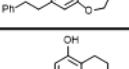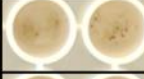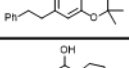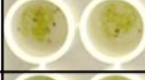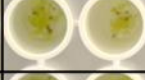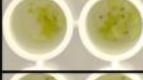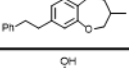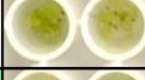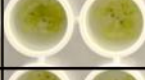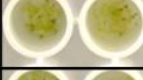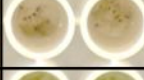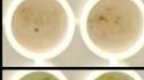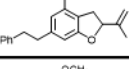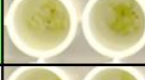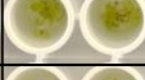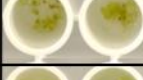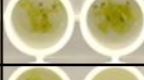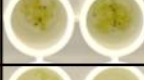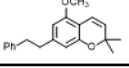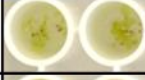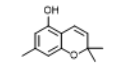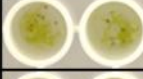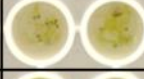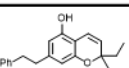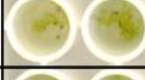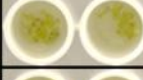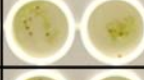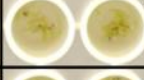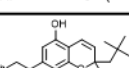
Figure 1

Figure 2

Figure 3

A

B

Figure 4

Figure 5

A

Legend:
- Control
- Radulanin A
- DCMU
- Bromoxynil

Y-axis: Relative TL intensity (0.0, 0.5, 1.0, 1.5)
X-axis: Temperature (°C) (-50, 0, 50, 100)

B

Legend:
- Control
- Radulanin A
- Radula chromene
- *O-methylated chromene*

Y-axis: Relative TL intensity (0.0, 0.5, 1.0, 1.5)
X-axis: Temperature (°C) (-50, 0, 50, 100)

Figure 6